Supplementary material:

Computational mining of Janus Sc_2C-based MXene for spintronic, photocatalytic, and solar cell applications

Yinggan Zhang[1], Baisheng Sa[2,*], Naihua Miao[3], Jian Zhou[3] and Zhimei Sun[3,*]

[1]*College of Materials, Fujian Provincial Key Laboratory of Theoretical and Computational Chemistry, Xiamen University, Xiamen 361005, P. R. China*
[2]*Key Laboratory of Eco-materials Advanced Technology, College of Materials Science and Engineering, Fuzhou University, Fuzhou 350108, P. R. China*
[3]*School of Materials Science and Engineering, and Center for Integrated Computational Materials Science, International Research Institute for Multidisciplinary Science, Beihang University, Beijing 100191, P. R. China*

Corresponding authors: bssa@fzu.edu.cn (B. Sa), zmsun@buaa.edu.cn (Z. Sun).

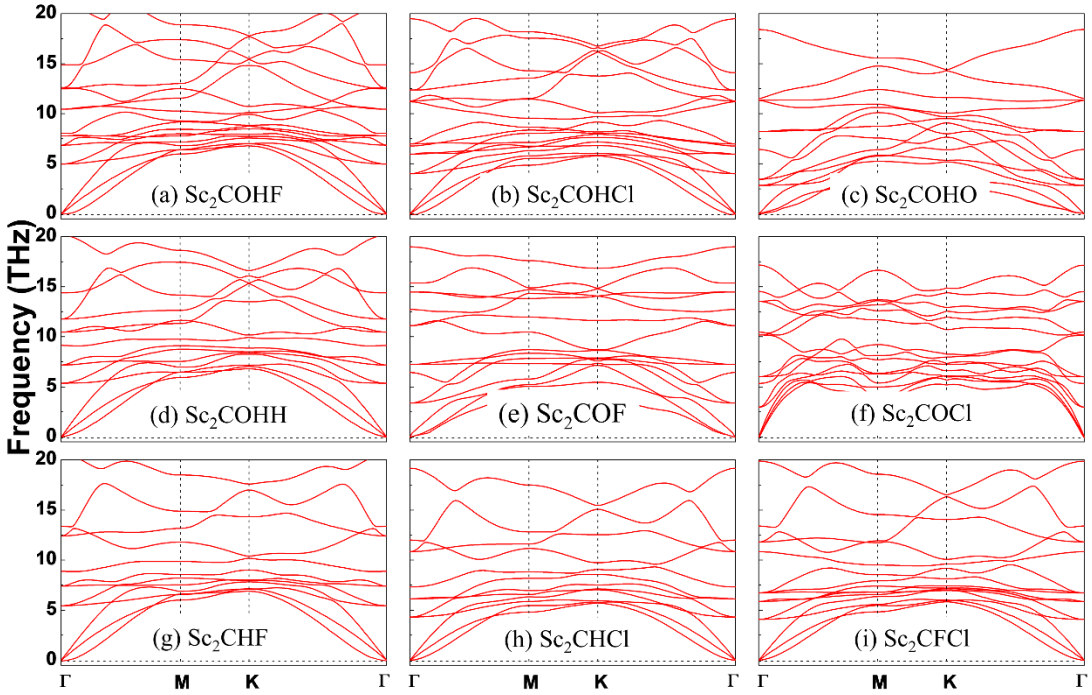

Fig. S1 Phonon dispersion curves for (a) Sc_2COHF, (b) Sc_2COHCl, (c) Sc_2COHO, (d) Sc_2COHH, (e) Sc_2COF, (f) Sc_2COCl, (g) Sc_2CHF, (h) Sc_2CHCl, (i) Sc_2CFCl.

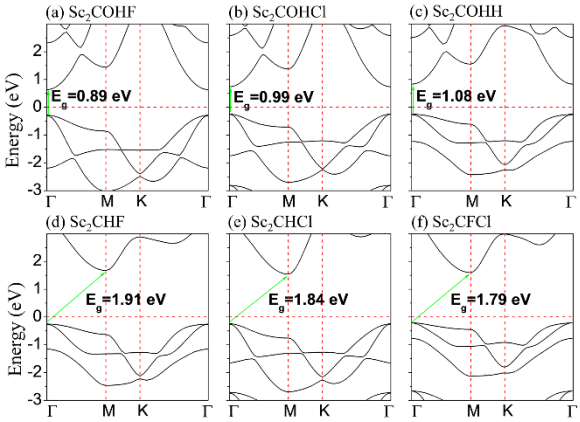

Fig. S2 The HSE06 band structures of Janus (a) Sc_2COHF, (b) Sc_2COHCl, (c) Sc_2COHH, (d) Sc_2CHF, (e) Sc_2HCl, (f) Sc_2CFCl.

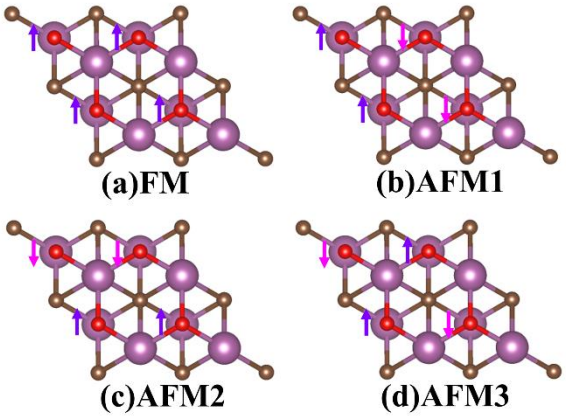

Fig. S3 Various possible magnetic configurations of Sc_2CTT' including (a) one ferromagnetic state and (b-d) three antiferromagnetic states with up-spins (↑) and down-spins (↓) on the Sc atom.

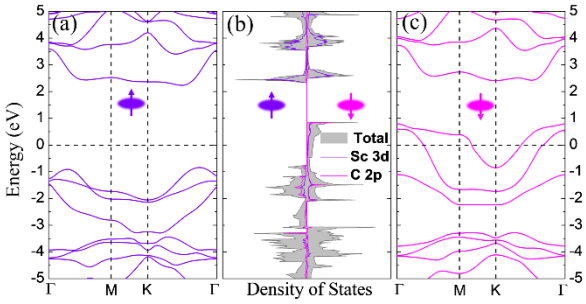

Fig. S4 The band structure of Sc_2COF with (a) spin-up and (c) spin-down states, and (b) the spin-resolved density of states. The Fermi level is set at 0 eV as indicated by a dashed line.

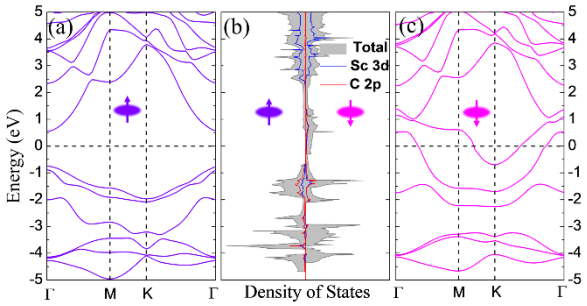

Fig. S5 The band structure of Sc_2COH with (a) spin-up and (c) spin-down states, and (b) the spin-resolved density of states. The Fermi level is set at 0 eV as indicated by a dashed line.

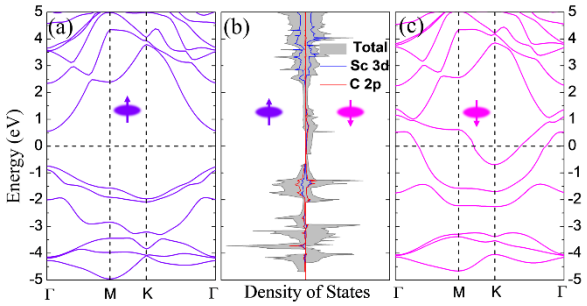

Fig. S6 The band structure of Sc_2COOH with (a) spin-up and (c) spin-down states, and (b) the spin-resolved density of states. The Fermi level is set at 0 eV as indicated by a dashed line.

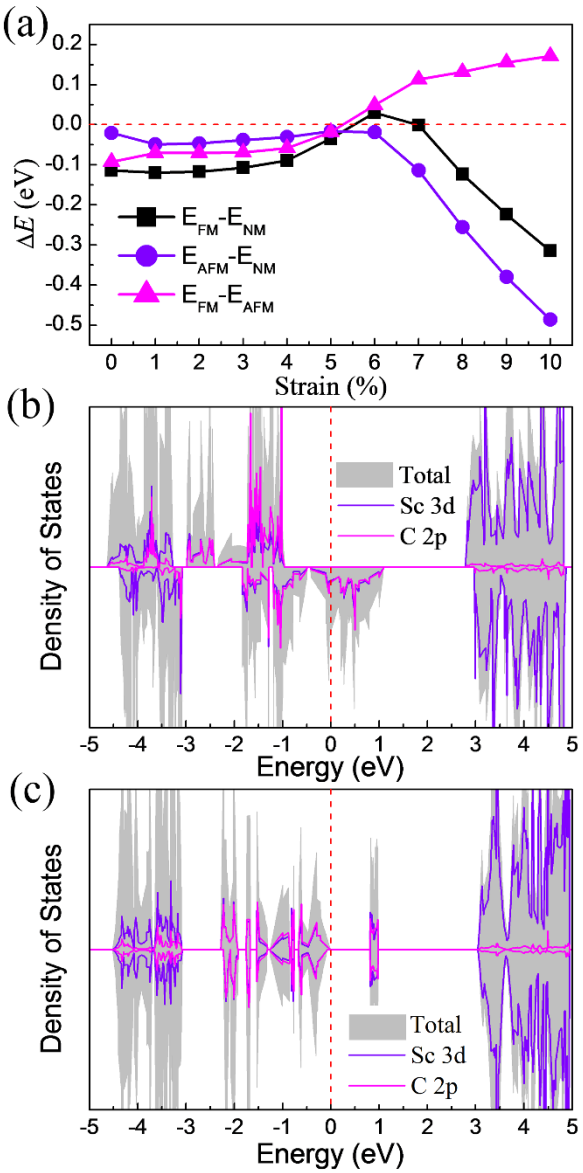

Fig. S7 (a) The energy differences between FM, AFM and NM states of Sc_2COF as a function of tensile strain. The spin-resolved density of states of Sc_2COF under (b) 5% tensile strain for FM states and (c) 6% tensile strain for AFM states, respectively.

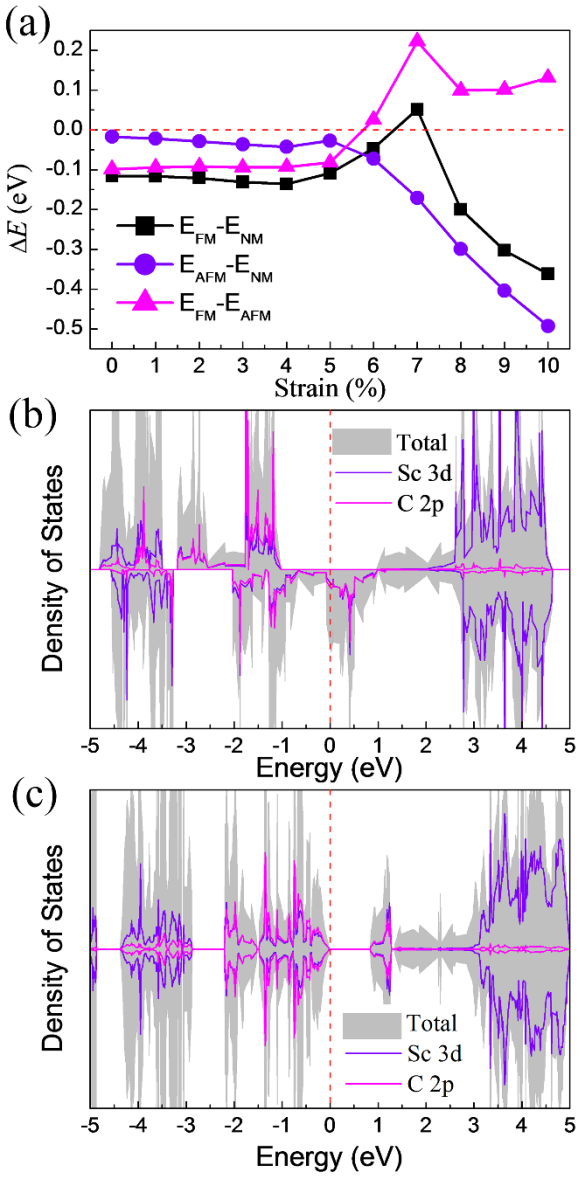

Fig. S8 (a) The energy differences between FM, AFM and NM states of Sc_2COOH as Fa function of tensile strain. The spin-resolved density of states of Sc_2COOH under (b) 5% tensile strain for FM states and (c) 6% tensile strain for AFM states, respectively.

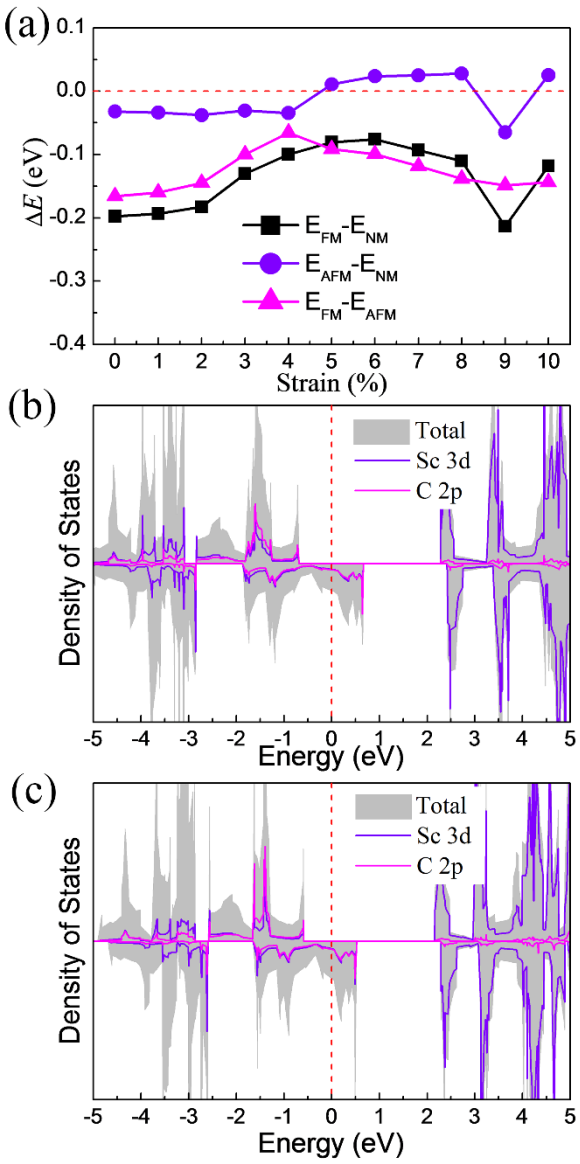

F

Fig. S9 (a) The energy differences between FM, AFM and NM states of Sc_2COH as a function of tensile strain. The spin-resolved density of states of Sc_2COH under (b) 5% and (c) 10% tensile strain for FM states, respectively.

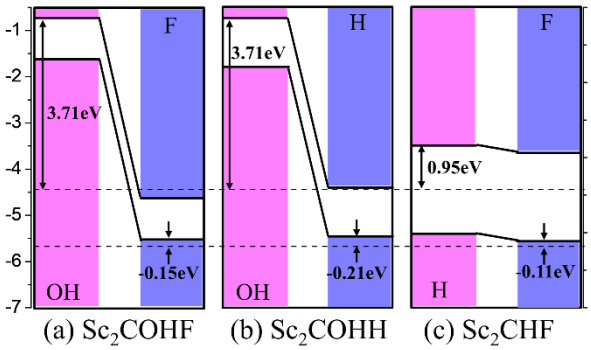

Fig. S10 Band alignment of (a) Sc_2COHF, (b) Sc_2COHH and (c) Sc_2CHF with respect to the redox potentials of water.

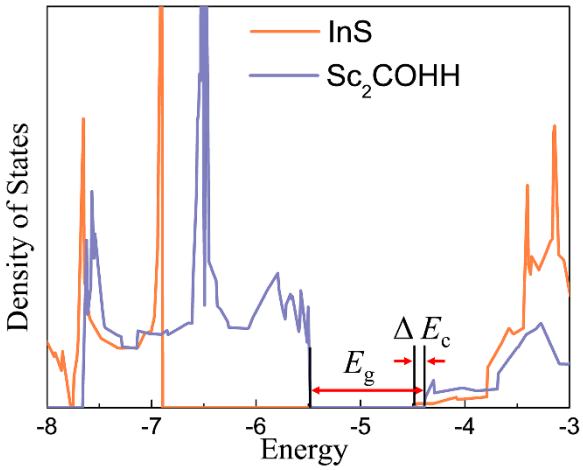

Fig. S11 The density of states of Sc_2COHH/InS heterostructure.